

The Use of Liquid–Liquid Interface (Biphasic) for the Preparation of Benzenetricarboxylate Complexes of Cobalt and Nickel

Abhishek Banerjee,^[a] Partha Mahata,^[a] and Srinivasan Natarajan^{*[a]}

Keywords: Metal–organic frameworks / Cobalt / Nickel/ Biphasic synthesis method

New metal–organic frameworks (MOFs) [Ni(C₁₂N₂H₁₀)(H₂O)] [C₆H₃(COO)₂(COOH)] (**I**), [Co₂(H₂O)₆] [C₆H₃(COO)₃]₂·(C₄N₂H₁₂)(H₂O)₂ (**II**), [Ni₂(H₂O)₆] [C₆H₃(COO)₃]₂·(C₄N₂H₁₂)(H₂O)₂ (**III**), [Ni(C₁₃N₂H₁₄)(H₂O)] [C₆H₃(COO)₂(COOH)] (**IV**), [Ni₃(H₂O)₈] [C₆H₃(COO)₃] (**V**) and [Co(C₄N₂H₄)(H₂O)] [C₆H₃(COO)₃] (**VI**) {C₆H₃(COOH)₃ = trimesic acid, C₁₂N₂H₁₀ = 1,10-phenanthroline, C₄N₂H₁₂ = piperazine dication, C₁₃N₂H₁₄ = 1,3-bis(4-pyridyl)propane and C₄N₂H₄ = pyrazine} have been synthesized by using an interface between two immiscible solvents, water and cyclohexanol. The compounds are constructed from the connectivity between the octahedral M²⁺ (M = Ni, Co) ions coordinated by oxygen atoms of carboxylate groups and water molecules and/or by

nitrogen atoms of the ligand amines and the carboxylate units to form a variety of structures of different dimensionality. Strong hydrogen bonds of the type O–H···O are present in all the compounds, which give rise to supramolecularly organized higher-dimensional structures. In some cases $\pi\cdots\pi$ interactions are also observed. Magnetic studies indicate weak ferromagnetic interactions in **I**, **IV** and **V** and weak antiferromagnetic interactions in the other compounds (**II**, **III** and **VI**). All the compounds have been characterized by a variety of techniques.

(© Wiley-VCH Verlag GmbH & Co. KGaA, 69451 Weinheim, Germany, 2008)

Introduction

Metal–organic frameworks (MOFs) have been in the forefront of research for their applications in the areas of adsorption,^[1] separation and catalysis.^[2] Additionally, the ability to incorporate almost all the elements of the periodic table along with the possibility of introducing functionality through the organic linkers provide the added impetus for the continuing interest.^[3] Of the many MOFs that have been synthesized,^[4] those with transition metals are important.^[5] The transition elements, with their varied oxidation states and coordination preferences, present an excellent opportunity to correlate magnetic, spectroscopic and related properties with the framework structure.^[6] The organic linkers, with varying lengths and functionalities, can form MOFs with adjustable channels and impart chemical reactivity and in some cases chirality.^[7]

A detailed study of the available literature clearly reveals that the number of metal–organic framework compounds formed by aromatic carboxylates is far more than that formed by aliphatic ones.^[4e,8] Of the many aromatic carboxylic acid based MOFs, those of trimesic acid^[9,10] (ben-

zene-1,3,5-tricarboxylic acid, H₃tma) form the largest number of high-symmetry structures.^[10] Most of these compounds are prepared by using a mild hydrothermal reaction between a metal salt, trimesic acid and a base.^[10a,10b,10d] Recently, there have been many attempts to modify the synthesis conditions, which has given rise to newer approaches, such as the biphasic solvothermal method^[12] and those that use ionic liquids,^[11] etc. Of these, the biphasic approach appears to have distinct advantages. In biphasic reactions, the metal salt is generally in aqueous medium and the organic acid is in an organic solvent, which is usually immiscible with water (cyclohexanol). The formation of the product phase is usually at or near the interface between the two liquids. This approach has been employed profitably for the preparation of many inorganic–organic hybrid compounds by Cheetham and co-workers.^[12] Recently, the liquid–liquid interface has also been employed for the synthesis of nanoparticles, nanocrystals, etc.^[13]

The biphasic synthesis is advantageous while working with metals that have low reduction potentials, i.e. metals that are easily reducible – as is the case for Cu²⁺ ions.^[12b] It also offers the possibility to work with organic solvents that may be unstable under hydrothermal conditions. Yaghi and co-workers employed a modified approach for the preparation of MOFs of aromatic dicarboxylates by employing two different solvents. Thus, Zn(NO₃)₂·6H₂O and naphthalene-2,6-dicarboxylic acid were dissolved in a mix-

[a] Framework Solids Laboratory, Solid State and Structural Chemistry Unit, Indian Institute of Science, Bangalore 560 012, India

E-mail: snatarajan@sscu.iisc.ernet.in

Supporting information for this article is available on the WWW under <http://www.eurjic.org> or from the author.

ture of diethyl formamide (def) and chlorobenzene (ClBz), and the solution was kept at room temperature without contact in a vessel containing def and triethylamine (tea). This approach resulted in isolating a new framework structure, $Zn_2[C_{10}H_8(COO)_2] \cdot [(Htea)(def)(ClBz)]_2$.^[14] In addition, they used a mixture of miscible solvents to crystallize related metal–organic frameworks.^[14] This approach, although it uses a variety of organic solvents, cannot truly be considered a biphasic method, since the solvents employed are generally miscible.

Though the biphasic method is seemingly advantageous, this approach for the preparation of inorganic–organic hybrid compounds has not caught the imagination of researchers. We sought to use this technique, in an exploratory way, for the preparation of benzenecarboxylates of cobalt and nickel. Our studies have been successful, and we have prepared six new compounds: $[Ni(C_{12}N_2H_{10})(H_2O)][C_6H_3(COO)_2(COOH)]$ (**I**), $[M_2(H_2O)_6][C_6H_3(COO)_3]_2 \cdot (C_4N_2H_{12})(H_2O)_2$ { $M = Co^{II}$ (**II**), Ni^{II} (**III**)}, $[Ni(H_2O)(C_{13}N_2H_{14})][C_6H_3(COO)_2(COOH)]$ (**IV**), $[Ni_3(H_2O)_8][C_6H_3(COO)_3]_2$ (**V**) and $[Co(C_4N_2H_4)(H_2O)][C_6H_3(COO)_2(COOH)]$ (**VI**). 1,10-Phenanthroline was used for **I**, piperazine for **II** and **III**, 1,3-bis(4-pyridyl)propane for **IV** and pyrazine for **VI**, whereas **V** was synthesized without any N-containing ligand. The compounds have 1D (**I**, **II**, **III** and **IV**) and 2D (**V** and **VI**) extended structures. In this paper, the synthesis, structure and properties of the compounds are presented.

Results and Discussion

Structures Description

$[Ni(C_{12}N_2H_{10})(H_2O)][C_6H_3(COO)_2(COOH)]$

The asymmetric unit of **I** consists of 35 non-hydrogen atoms with one Ni^{2+} ion that is crystallographically independent. The Ni^{2+} ion has a distorted octahedral geometry, which is formed by three carboxylate oxygen atoms, two nitrogen atoms of the phenanthroline ring and a bound water molecule. The Ni–O/N bonds have lengths in the range 2.021–2.148 Å (av. 2.08 Å) and the O/N–Ni–O/N bond angles are in the range 77.9(1)–173.0(1)° (Table 1). The structure consists of two $NiO_3N_2(H_2O)$ octahedra connected through two μ_3 carboxylate oxygen atoms [O(3)] (μ_3 -O connected to two Ni^{+2} ions and one carbon atom) to form an edge-shared dimer. The dimers are connected by [Htma]²⁻ ligands to form a ladderlike one-dimensional structure (Figure 1a). The structure is stabilized by hydrogen-bond interactions and $\pi \cdots \pi$ interactions between [Htma]²⁻ and 1,10-phenanthroline molecules. Strong O–H \cdots O hydrogen-bond interactions between the bonded water molecules and the carboxylate oxygen atoms give rise to a supramolecularly organized two-dimensional structure along the *c* axis (Figure 1b). The important hydrogen-bond interactions are given in Table 2. This structure is closely related to the cobalt compound $[Co(C_{12}N_2H_{10})(H_2O)][C_6H_3(COO)_2(COOH)]$ reported previously.^[15]

Table 1. Selected bond lengths in compounds **I–IV** and **VI**.^[a]

Bond	Distance [Å]	Bond	Distance [Å]
I			
Ni(1)–O(1)	2.021(3)	Ni(1)–O(3)#1	2.148(3)
Ni(1)–O(2)	2.046(3)	Ni(1)–N(1)	2.063(3)
Ni(1)–O(3)	2.093(3)	Ni(1)–N(2)	2.093(3)
II			
Co(1)–O(1)#1	2.0788(15)	Co(2)–O(4)	2.041(2)
Co(1)–O(1)	2.0788(15)	Co(2)–O(4)#2	2.041(2)
Co(1)–O(2)#1	2.0927(16)	Co(2)–O(5)#2	2.1161(16)
Co(1)–O(2)	2.0927(16)	Co(2)–O(5)	2.1161(16)
Co(1)–O(3)#1	2.1205(16)	Co(2)–O(6)#2	2.1776(16)
Co(1)–O(3)	2.1205(16)	Co(2)–O(6)	2.1776(16)
III			
Ni(1)–O(1)#1	2.043(3)	Ni(2)–O(4)	2.046(4)
Ni(1)–O(1)	2.043(3)	Ni(2)–O(4)#2	2.046(4)
Ni(1)–O(2)#1	2.057(3)	Ni(2)–O(5)#2	2.076(3)
Ni(1)–O(2)	2.057(3)	Ni(2)–O(5)	2.076(3)
Ni(1)–O(3)#1	2.085(3)	Ni(2)–O(6)#2	2.129(3)
Ni(1)–O(3)	2.085(3)	Ni(2)–O(6)	2.129(3)
IV			
Ni(1)–O(1)	1.997(2)	Ni(1)–O(4)	2.137(2)
Ni(1)–O(2)	2.072(2)	Ni(1)–N(1)	2.065(3)
Ni(1)–O(3)	2.120(2)	Ni(1)–N(2)	2.103(3)
VI			
Co(1)–O(1)	2.009(4)	Co(1)–O(4)	2.243(4)
Co(1)–O(2)	2.026(4)	Co(1)–N(1)	2.182(5)
Co(1)–O(3)	2.136(4)	Co(1)–N(2)	2.185(5)

[a] Symmetry transformations used to generate equivalent atoms – **I**: #1 $-x + 1, -y + 2, -z + 1$; **II** and **III**: #1 $-x + 1, -y + 1, -z + 1$; #2 $-x + 1, -y, -z$.

$[M_2(H_2O)_6][C_6H_3(COO)_3]_2 \cdot (C_4N_2H_{12})(H_2O)_2$ ($M = Co^{II}, Ni^{II}$)

The compounds **II** (Co) and **III** (Ni) are isostructural and have 24 non-hydrogen atoms in the asymmetric unit. There are two crystallographically independent M^{2+} ions, both of them are octahedrally coordinated and occupy special positions [M(1) at site 1b and M(2) at site 1c with a site multiplicity of 0.5], and one complete trimesate anion. M(1) has two carboxylate oxygen atoms [O(1)] and four water molecules [O(2), O(3)], and M(2) has two water molecules [O(6)] and four carboxylate oxygen atoms [O(4), O(5)] completing the octahedral coordination. The M–O bonds have lengths in the range 2.041(2)–2.178(2) Å (av. 2.105 Å for **II** and 2.072 Å for **III**), and the O–M–O bond angles are in the range 61.3(6)–180.0° (Table 1). Although the majority of the planar angles are close to 90° (ideal value for the octahedral coordination), the angle O(5)–M(2)–O(6) is 61.3(6)°, which leads to distortions. The M(2)–O(5) and M(2)–O(6) bonds are also relatively longer (Table 1). The single-crystal structures of both compounds have been reported earlier without any detailed description.^[16] Here, we describe the structures and also provide a detailed discussion of the weak interactions, such as hydrogen bond and $\pi \cdots \pi$ interactions. The trianionic trimesate units link the M^{2+} ions, which gives rise to an anionic one-dimensional structure (Figure 2a). The one-dimensional chains are arranged in an orthogonal fashion, which leads to a layerlike arrangement with void spaces (Figure 2b). The

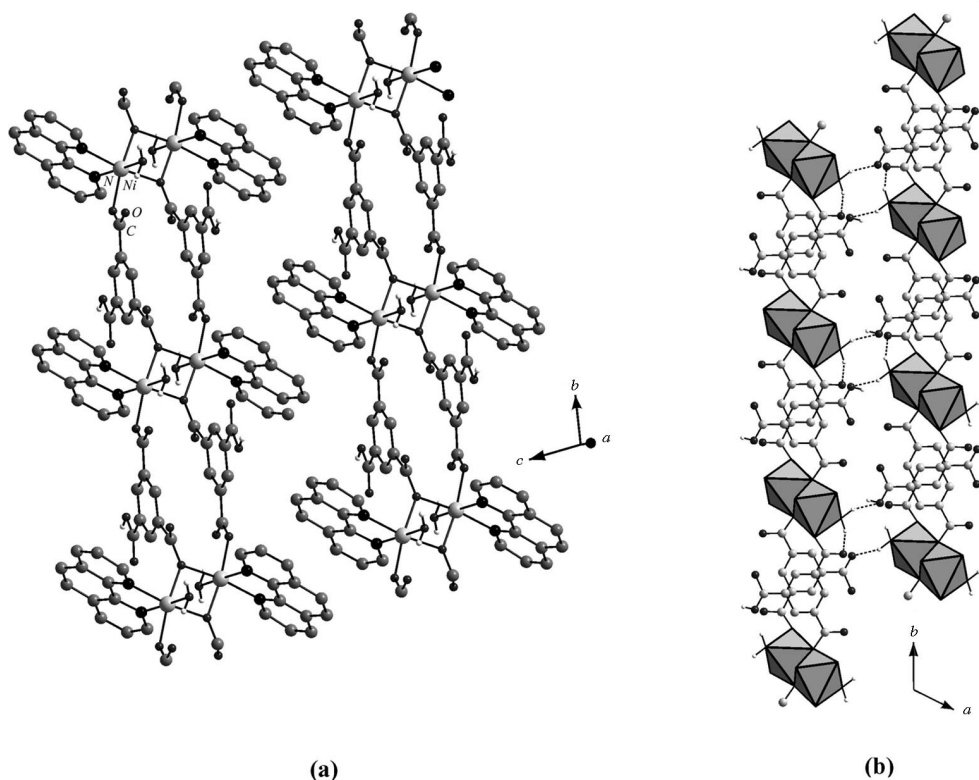


Figure 1. (a) The one-dimensional ladder in $[\text{Ni}(\text{C}_{12}\text{N}_2\text{H}_{10})(\text{H}_2\text{O})][\text{C}_6\text{H}_3(\text{COO})_2(\text{COOH})]$ (**I**). (b) Hydrogen-bond interactions between the coordinated water and the carboxylate oxygen atoms in **I**. The 1,10-phenanthroline molecules, bonded to the Ni^{2+} ions, have been omitted for clarity.

Table 2. Important H-bonding interactions present in compounds **I**, **II** and **VI**.^[a]

D–H...A	D–H [Å]	H...A [Å]	D...A [Å]	D–H...A [°]
I				
O(2)–H(2a)...O(4) ^[b]	0.94(5)	1.73(4)	2.625(5)	158(6)
O(2)–H(2a)...O(6)#1 ^[c]	0.94(4)	1.90(4)	2.778(5)	153(4)
II, III				
O(2)–H(2a)...O(6)#1	0.95(5)	1.81(6)	2.742(5)	165(7)
O(2)–H(2b)...O(8)#2	0.95(4)	1.71(4)	2.654(4)	170(4)
O(3)–H(3a)...O(7)	0.95(5)	1.75(5)	2.628(5)	152(7)
O(3)–H(3b)...O(8)#3	0.94(5)	1.81(6)	2.716(4)	162(6)
O(4)–H(4a)...O(7)#4	0.96(3)	1.75(3)	2.692(5)	169(6)
O(100)–H(102)...O(4)#5	0.89(3)	1.97(3)	2.809(8)	157(4)
C(12)–H(12a)...O(3)	0.97	1.99	2.892(5)	154
C(12)–H(12b)...O(9)#6	0.97	1.78	2.728(6)	165
VI				
O2...H2A...O6#1	0.95(8)	1.77(7)	2.697(7)	165(7)
O2...H2B...O4#2	0.95(9)	1.77(9)	2.695(6)	164(11)

[a] Symmetry transformations used to generate equivalent atoms – **I**: #1 $-1 + x, -1 + y, z$; **II**: #1 $1 - x, -y, 1 - z$; #2 $1 + x, 1 + y, z$; #3 $x, 1 + y, z$; #4 $x, y, 1 + z$; #5 $-x, -y, 2 - z$; #6 $1 + x, 1 + y, z$; **VI**: #1 $x, 1 + y, z$; #2 $-x, 1 - y, -z$. [b] Intramolecular. [c] Intermolecular.

void is occupied by charge compensating protonated piperazine and water molecules (Figure 2b). The presence of bonded and lattice water molecules in close proximity gives rise to O–H...O type hydrogen bonds (Figure 3a, Table 2). In addition π ... π interactions between the benzene rings are also observed.

One of the notable features in the structure of **II** and **III** is the presence of cyclic water tetramer units. Hydrogen-bond interactions between the bound water [O(4)] and lattice water [O(100)] lead to a tetramer with an average O–O distance of 2.78 Å (Figure 3a, b). Formation of water clusters of different shapes and sizes has been an important feature in many MOF compounds.^[17] The study of water clusters, especially the energies involved, are expected to provide valuable information regarding the role of the hydrogen-bond interactions in bulk water (ice) and in some MOF compounds and their role in the structural stability. Since the present compounds have low-dimensional character, such a study would be important to understand the role of hydrogen bonds in stabilizing such structures. To this end, we have performed some preliminary calculations on the stability of the water cluster using the Gaussian98 package.^[18] A single-point energy calculation was performed without symmetry constraints. A value of 27.41 kcal mol⁻¹ for the water tetramer was obtained, which is comparable with the values generally obtained for O–H...O hydrogen bonds.^[19] Since the water tetramer is formed from the bound as well as the lattice water, this energy may be important for the structural stability.

$[\text{Ni}(\text{H}_2\text{O})(\text{C}_{13}\text{N}_2\text{H}_{14})][\text{C}_6\text{H}_3(\text{COO})_2(\text{COOH})]$

Compound **IV** has 35 non-hydrogen atoms in the asymmetric unit. The crystallographically independent Ni^{2+} ion is surrounded by three carboxylate oxygen atoms, two nitro-

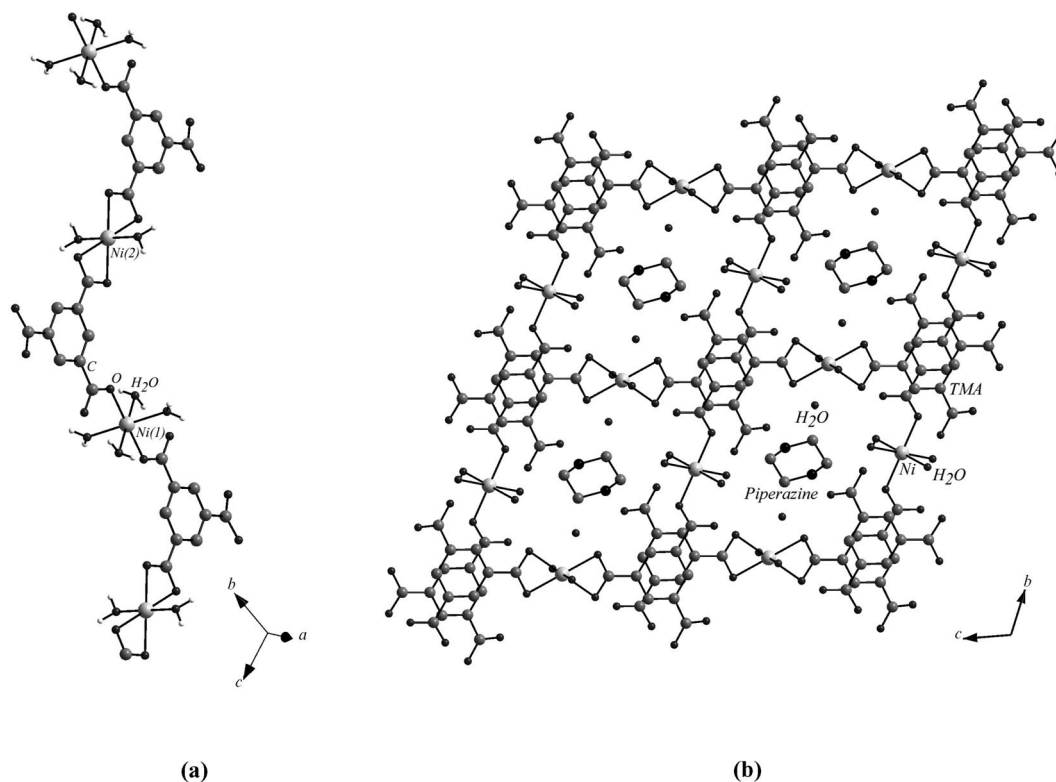


Figure 2. (a) The one-dimensional zig-zag chain in $[\text{Ni}_2(\text{H}_2\text{O})_6][\text{C}_6\text{H}_3(\text{COO})_3]_2 \cdot (\text{C}_4\text{N}_2\text{H}_{12})(\text{H}_2\text{O})_2$ (**III**). (b) Packing diagram of **III** showing the open apertures occupied by the piperazine and water molecules. H atoms have been omitted for clarity.

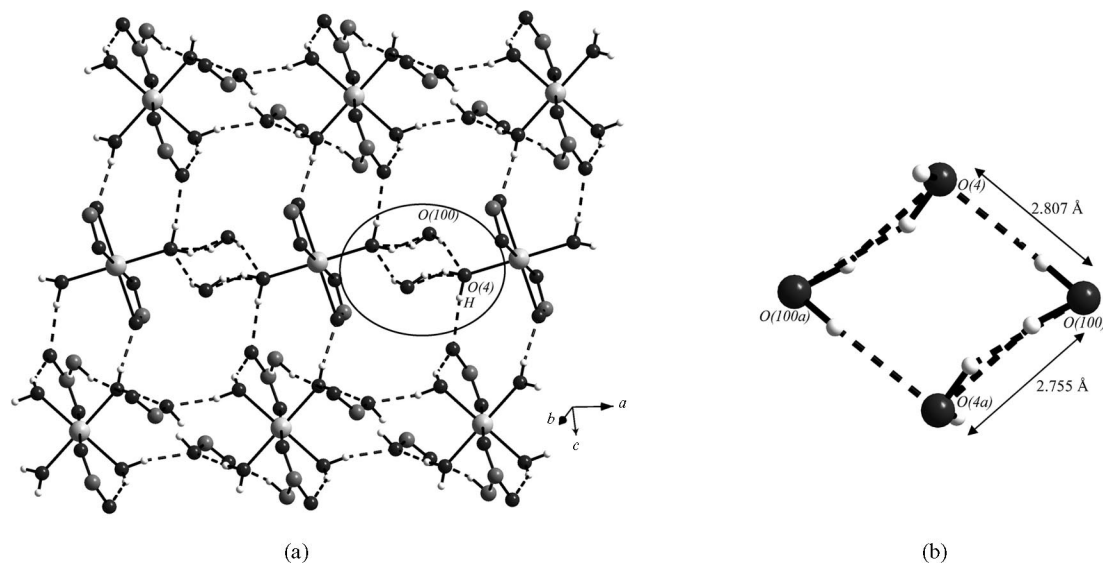


Figure 3. (a) View of hydrogen-bond interactions between the lattice water, the coordinated water and the C–O group of the carboxylate in **III**. Note the formation of a cyclic water tetramer by bonded and lattice water molecules (encircled). (b) View of the water tetramer.

gen atoms of 1,3-bis(4-pyridyl)propane (bpp) and a water molecule and has a distorted octahedral environment $[\text{Ni}(\text{H}_2\text{O})\text{O}_3\text{N}_2]$. There is one trimesate unit in the structure, which is dianionic, and one bis(pyridyl)propane unit. The Ni–O/N bonds have lengths in the range 1.997(2)–2.138(2) Å (av. 2.083 Å), and the O/N–Ni–O/N bond angles are in the range 61.8(7)–178.9(1)° (Table 1). The structure is composed of linkages between the Ni^{2+} ions, two dianionic

trimesate anions and one bpp unit to give rise to a one-dimensional ladderlike structure that resembles a column. The dianionic trimesate groups can be classified into two different types on the basis of their coordination with metal ions; in acid-1, two carboxylate groups are bidentately connected to Ni^{2+} , and in acid-2, two carboxylate groups are monodentately connected. The NiO_4N_2 octahedra are connected to two bpp units to form a dimer, which is connected

by acid-1 and acid-2 alternatively to form a columnlike arrangement as shown in Figure 4a. The columns are supramolecularly organized through strong O–H⋯O hydrogen bonds involving the free –COOH group of the trimesate dianion, with average O–O contact distances of 2.6 Å (Figure 4b). Although –COOH dimers have been well established in supramolecularly organized organic compounds,^[20] this is the first example of such interactions forming a three-dimensional structure through columns in a metal–organic framework system.

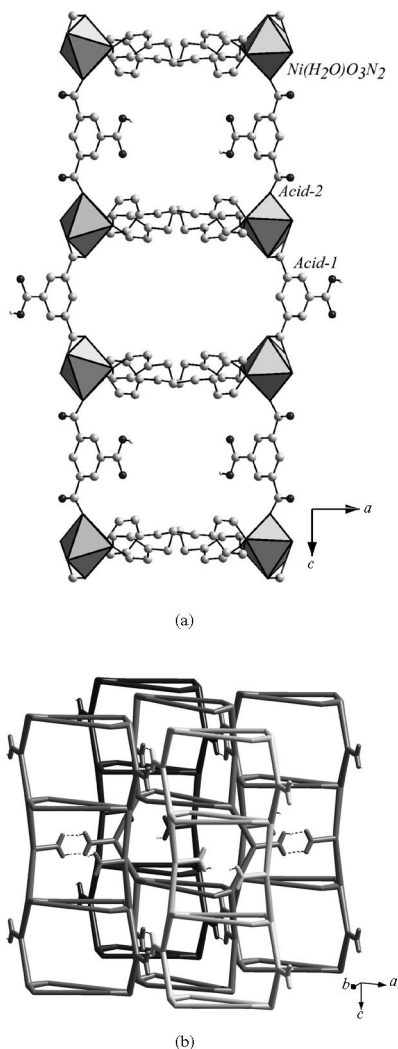


Figure 4. (a) The one-dimensional columnlike structure in $[\text{Ni}(\text{C}_{13}\text{N}_2\text{H}_{14})(\text{H}_2\text{O})][\text{C}_6\text{H}_3(\text{COO})_2(\text{COOH})]$ (IV). Note the presence of two different types of carboxylic acid groups. (b) Schematic diagram showing the arrangements of four different columns around a single column, with all possible hydrogen-bonding interactions shown.



This compound has 42 non-hydrogen atoms in the asymmetric unit, with four crystallographically independent Ni^{2+} ions and two trimesate anions. The coordination geometry

around the Ni^{2+} ions is similar to that observed in compound III. The Ni–O bonds have lengths in the range 2.029(2)–2.139(2) Å (av. 2.068 Å), and the O–Ni–O bond angles are in the range 81.1(1)–180.0°. Two sets of Ni species [Ni(1) and Ni(3), and Ni(2) and Ni(4)] are connected through μ_2 -OH₂ and carboxylate bridges to form a trinuclear unit, which are linked by the trimesate anions to give rise to a two-dimensional layer (Figure 5). This compound has recently been isolated through a complex synthesis procedure,^[21] and hence no further discussion will be provided here.

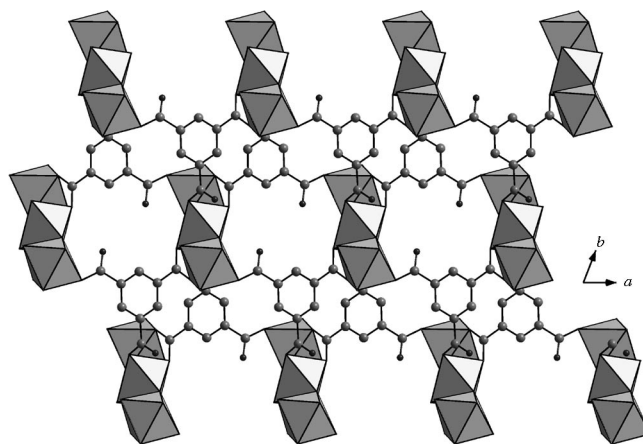


Figure 5. View of the two-dimensional structure formed through the connectivity between the Ni^{2+} trimeric unit and the tma ligands in $[\text{Ni}_3(\text{H}_2\text{O})_8][\text{C}_6\text{H}_3(\text{COO})_3]$ (V).



Compound VI has 23 non-hydrogen atoms in the asymmetric unit. The crystallographically independent Co^{2+} ion is surrounded by three carboxylate oxygen atoms, two nitrogen atoms of pyrazine and a water molecule, which forms a distorted octahedral environment, $[\text{Co}(\text{H}_2\text{O})\text{O}_3\text{N}_2]$. The coordination environment around the Co^{2+} ions is similar to that observed around the Ni^{2+} ions in IV. The Co–O/N bonds have lengths in the range 2.009(4)–2.243(4) Å (av. 2.13 Å) (Table 1), and the O/N–Co–O/N bond angles are in the range 59.8(2)–178.2(2)° (Table S6). The small O(1)–Co–O(2) bond angle is due to the bidentate nature of one of the carboxylate groups towards the Co^{2+} ion. The connectivity between the Co^{2+} ions and the trimesate $[\text{Htma}]^{2-}$ units leads to one-dimensional chains, which are connected by pyrazine ligands to form the two-dimensional structure with a 4,4-net topology (Figure 6a). The adjacent layers are turned 180° relative to the first layer and results in an ABAB-type layer arrangement (Figure 6b). The layers are supramolecularly connected through hydrogen-bond interactions to form a pseudo-three-dimensional structure (Figure S1, Table 2).

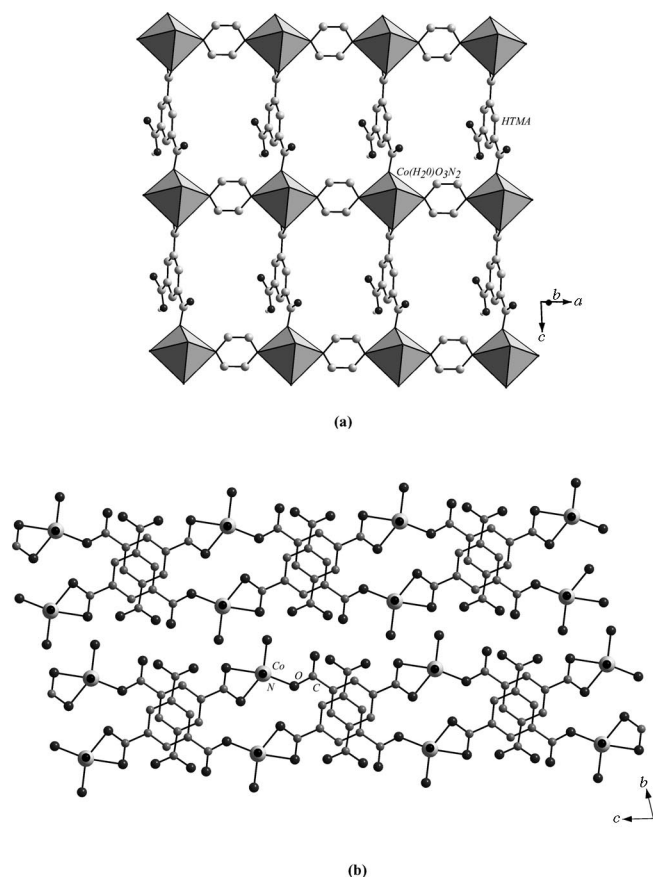


Figure 6. (a) The two-dimensional structure of $[\text{Co}(\text{C}_4\text{N}_2\text{H}_4)(\text{H}_2\text{O})][\text{C}_6\text{H}_3(\text{COO})_2(\text{COOH})]$ (VI). Note the (4,4) nets. (b) The stacking of the layers in the bc plane. Note that the layers are arranged in an ABAB... fashion.

Structural Comparison

All the structures obtained in the present study are formed with trimesate anions, which are variably deprotonated. The structural features of compounds I–VI can be compared and contrasted with other similar structures formed using trimesic acid. Thus, I has a similar structure to that of $[\text{Co}(\text{C}_{10}\text{N}_2\text{H}_8)(\text{H}_2\text{O})][\text{C}_6\text{H}_3(\text{COO})_2(\text{COOH})]$.^[22] In I, the secondary chelation occurs with 1,10-phenanthroline and in $[\text{Co}(\text{C}_{10}\text{N}_2\text{H}_8)(\text{H}_2\text{O})][\text{C}_6\text{H}_3(\text{COO})_2(\text{COOH})]$ with 2,2'-bipyridine.^[22] The structures of II and III, although appear to be unique in their arrangement, can be correlated with the structure of $[\text{M}_3(\text{H}_2\text{O})_{12}][\text{C}_6\text{H}_3(\text{COO})_3]_2$ (M = Co, Ni, Zn) reported by Yaghi and co-workers (Figure 7a).^[23] The overall connectivity in II and III and in the structure reported by Yaghi and co-workers are comparable; the compounds have one-dimensional structures that exhibit strong hydrogen-bonding interactions, which give rise to channel structures. Unlike the structure reported by Yaghi and co-workers,^[23] in II and III, the channels are not empty but are occupied by piperazinium cations and water molecules. The void space, thus, in II and III are fully occupied and also gives rise to cyclic water tetramer units. In the structure of Yaghi and co-workers,^[23] the void space creates opportunities for the reversible adsorption behav-

our. In this compound, the metal and the trianionic trimesate units are in the ratio 3:2, and their connectivity gives rise to a neutral one-dimensional chain structure, stabilized by O–H...O hydrogen bonds. In II and III, the metal and the trimesate units are in the ratio 1:1, and their connectivity results in a one-dimensional structure, which is anionic. Charge balance is achieved by the incorporation of protonated piperazine molecules, which lead to additional hydrogen-bond interactions, which are absent in $[\text{M}_3(\text{H}_2\text{O})_{12}][\text{C}_6\text{H}_3(\text{COO})_3]_2$ (M = Co, Ni, Zn).^[23]

The structure of IV appears to have a close resemblance to $[\text{Cd}(\text{C}_{13}\text{N}_2\text{H}_{14})_2][\text{CH}_3(\text{COO})_2(\text{COOH})]$ (Figure 7b).^[24] In both the structures, we have $[\text{Htma}]^{2-}$ and one free –COOH group. The one-dimensional chains formed by Cd^{2+} and the $[\text{Htma}]^{2-}$ ions are similar to those observed in IV (Figure 7b). In IV, the bpp ligands connect two chains to form a unique one-dimensional columnlike structure (Figure 4a), whereas in the Cd compound, the bpp ligands are bonded along the opposite side of each chain to form a simple two-dimensional layer structure (Figure 7b). The structure of VI is similar to $[\text{Ni}_2(\text{C}_{10}\text{N}_2\text{H}_8)(\text{H}_2\text{O})][\text{C}_6\text{H}_3(\text{COO})_2(\text{COOH})]$ reported earlier (Figure 7c).^[25] A gridlike structure consisting of two Ni–tma chains connected by 4,4'-bipyridine has been observed in $[\text{Ni}_2(\text{C}_{10}\text{N}_2\text{H}_8)(\text{H}_2\text{O})][\text{C}_6\text{H}_3(\text{COO})_2(\text{COOH})]$, whereas the pyrazine molecule connects the Co centres in VI. The smaller linker pyrazine gives rise to a shorter Co–Co distance (7.14 Å) than the Ni–Ni distance in the nickel compound $[\text{Ni}_2(\text{C}_{10}\text{N}_2\text{H}_8)(\text{H}_2\text{O})][\text{C}_6\text{H}_3(\text{COO})_2(\text{COOH})]$ (11.25 Å) (Figure 7c).

Role of Weak Interactions

The use of hydrogen bonding in inorganic crystal design has been of much focus recently.^[26] A hydrogen bond of the type D–H...A can be broadly defined as one that requires a donor (D) that forms a polar σ bond with hydrogen (D–H) and interacts through the hydrogen atom in an attractive manner with at least one acceptor atom or group (A) by virtue of a lone pair of electrons or other accumulation of electron density on the acceptor (A). Thus, a hydrogen bond is an interaction between a Lewis acid and a Lewis base, wherein D–H serves as a Lewis acid and A as the Lewis base. When considering the hydrogen bonds in inorganic systems, the strength of the hydrogen-bond interactions, the reliability of the hydrogen-bonded recognition motifs and the attainability of a particular hydrogen bond may be important. To this end, the definitions for a variety of hydrogen bonds provided by Desiraju and Steiner^[20] is of considerable importance. For a D–H...O hydrogen bond (D, A = O or N) to be strong, the energies are likely to be in the range 4–15 kcal mol^{−1}. The strong hydrogen bonds can effectively participate through directed assembly of the building units. On the basis of the many structures available in the literature, the participating functional groups can be carbonyl, amide, oxime, alcohol, amine, etc. and the metals.^[26]

Many of the present structures are low-dimensional, and hydrogen-bond interactions play a key role in the stability

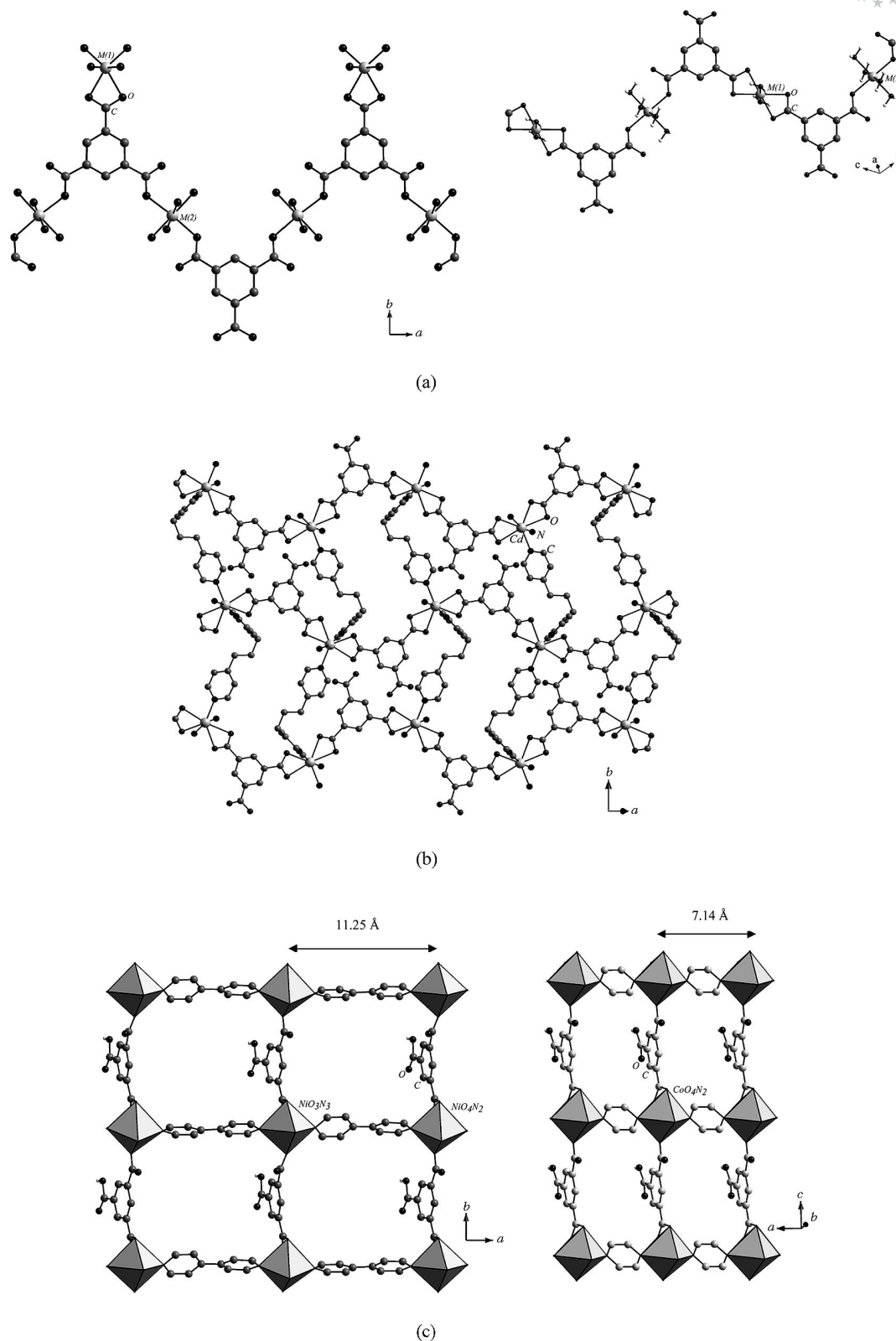


Figure 7. (a) The one-dimensional chain in $[M_3(H_2O)_{12}][C_6H_3(COO)_3]_2$ ($M = Co, Ni, Zn$) and in **III**. (b) View of the two-dimensional structure formed by the linking of Cd–tma chains by bpp ligands in $[Cd(C_{13}N_2H_{14})_2][CH_3(COO)_2(COOH)]$. (c) The two-dimensional gridlike structure of $[Ni_2(C_{10}N_2H_8)(H_2O)][C_6H_3(COO)_2(COOH)]$ and **VI**. Note the difference in the linking ligand (see text).

of such structures. Many hydrogen-bonded motifs involving carboxylate and/or amine/amide-based synthons have been well established and reported in the literature.^[27] Of these, we have observed the classic dimer motif along with a few

new ones that involve the water molecules. In **I** and **VI**, we observed an O–H···O interaction between the carboxylate group and the water molecules (Figure 8), where both the water hydrogen atoms act as the donor and one of the oxygen atoms of the carboxylate groups acts as the acceptor (Figure 8a). In **II** and **III**, we observed both O–H···O and C–H···O interactions (Figure 8b–d). The O–H···O interactions are different from those observed in **I** (Figure 8b); the acceptor oxygen atoms are different – one is a carboxylate oxygen atom and the other is a carboxylic acid oxygen atom. The C–H···O interaction is between the methylene hydrogen atom of the piperazine and the oxygen atom of the carboxylic acid group (Figure 8c). In **II** and **III**, the O–

H···O interactions also give rise to a cyclic water tetramer, which is noteworthy. The calculated energy of $27.41 \text{ kcal mol}^{-1}$ for the water clusters is within the range $15\text{--}40 \text{ kcal mol}^{-1}$ observed for very strong hydrogen bonds.^[19] The water clusters, formed by involving the lattice water and bound water molecules, give additional structural stability to **II** and **III**.

In **IV**, the free –COOH group of tma is primarily responsible for the formation of a supramolecularly organized three-dimensional structure. The hydrogen atom of the carboxylic acid group and the oxygen atom of the other carboxylic acid group interact to form the classical carboxylate dimer (Figure 8e). The observed O–O distance of 2.59 and

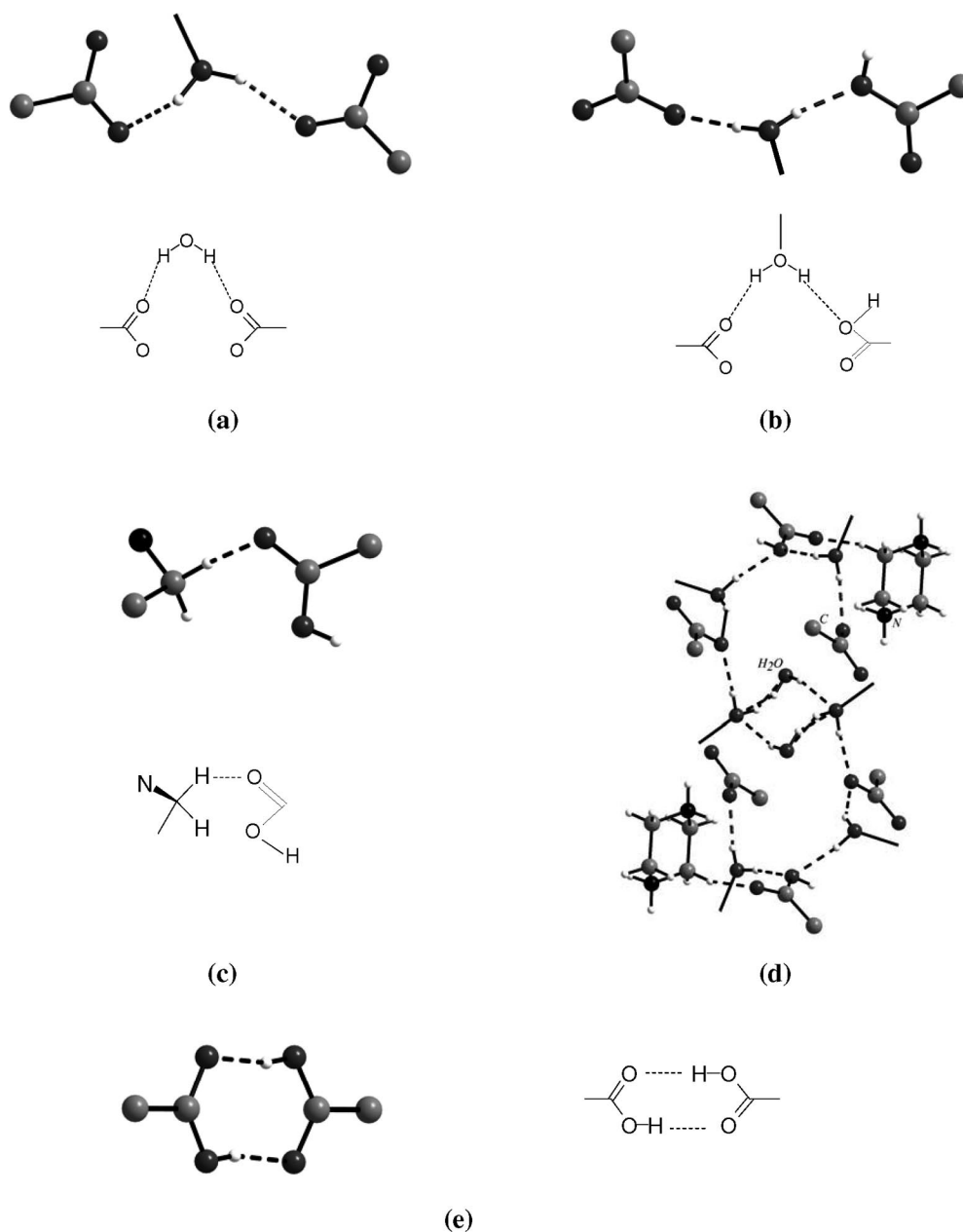


Figure 8. Representations of the hydrogen-bonding motifs observed in the present structures (a) **I** and **VI**, (b), (c), (d) **II** and **III** and (e) **IV**.

O–H \cdots O bond angle of 167° can be described as strong hydrogen bonds. A single column in **IV** connects through the carboxylate dimers to neighbouring columns to form the three-dimensional structure with sinusoidal spaces.

In addition to this, many of the structures are also stabilized by $\pi\cdots\pi$ interactions involving the benzene ring of the carboxylate groups. The role of $\pi\cdots\pi$ interactions in the stability of supramolecularly engineered crystal structures have been well documented and in recent years, the role of $\pi\cdots\pi$ interactions in extended structures has been a topic of much interest.^[28] In the present compounds, we find significant intermolecular $\pi\cdots\pi$ interactions between two aromatic rings of 1,10-phenanthroline in **I** and tma in **I**, **II**, **III** and **VI**. The centroid–centroid distance (d) and the interplanar angle (θ) between the 1,10-phenanthroline rings of **I** and between the tma units of **I**, **II** and **VI** are shown in Figure 9a–d, respectively. Favourable $\pi\cdots\pi$ interactions have been observed in these compounds as can be seen from Figure 9.

Strong $\pi\cdots\pi$ interactions are also observed in **VI**, where they are seen to act in a parallel direction to the two-dimensional sheet of **VI**. Most importantly, because of the short Co–Co distances, the connecting [Htma]²⁻ ions are close (3.683 and 3.805 Å), which results in two different $\pi\cdots\pi$ in-

teractions (Figure S2). It has been observed that the aromatic rings in tma in all the structures are parallel to each other but are staggered in conformation with respect to the carboxylate group. This staggered arrangement of the aromatic rings has been commonly observed in systems exhibiting dipolar properties. It is likely that the staggered arrangement of the tma anions reduces the dipole–dipole repulsion between the two carboxylate groups. The $\pi\cdots\pi$ interaction energy has been calculated by using the Gaussian98 software package at the [B3LYP/6-31 + G(d,p)] level of theory.^[18] The net $\pi\cdots\pi$ interactions calculated on the basis of the above arrangements of the carboxylate groups give rise to energies of 3.21, 3.94 and 3.45 and 3.25 kcal mol⁻¹ between the tma rings for **I**, **II** and **VI**, respectively, and to an energy of 1.24 kcal mol⁻¹ between the 1,10-phenanthroline rings for **I**. These are typical values and similar $\pi\cdots\pi$ interaction energies have been observed before.^[29]

Physical Properties

UV/Vis Spectroscopic Studies

The diffuse reflectance UV/Vis spectra at room temperature were recorded for the sodium salt of tma and for the

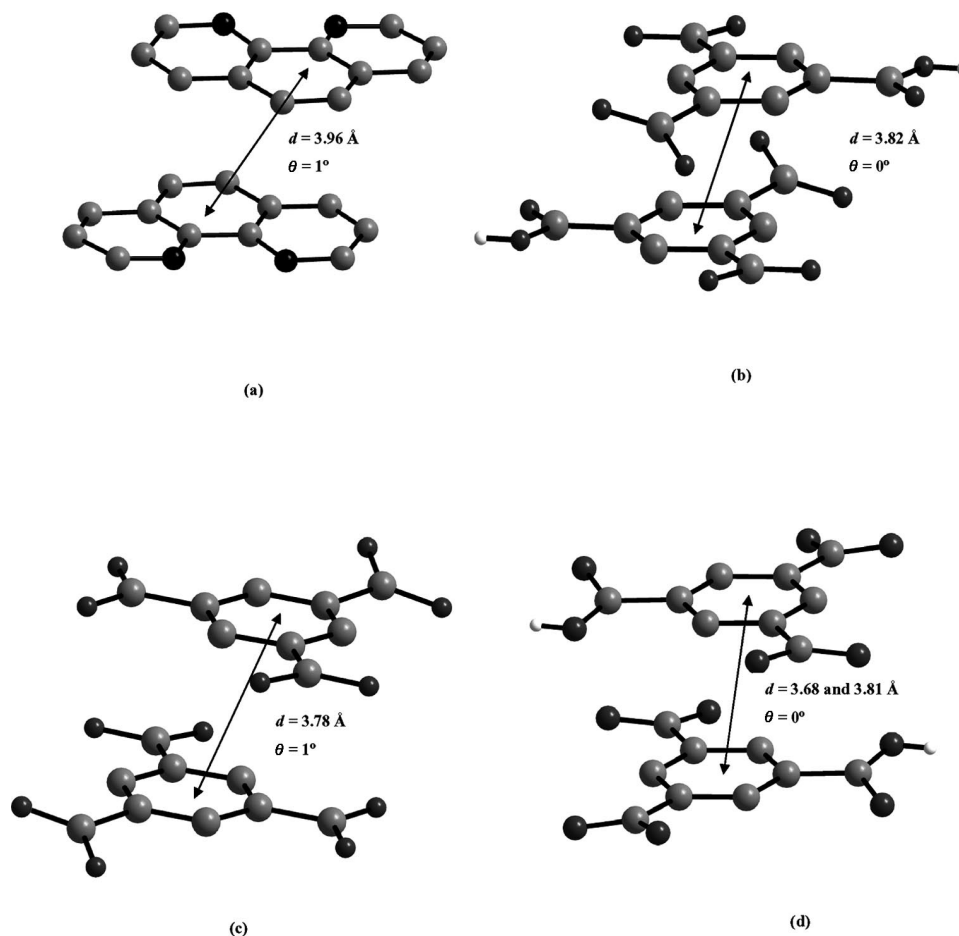


Figure 9. The possible $\pi\cdots\pi$ interaction between the (a) 1,10-phenanthroline ligands in **I**, (b) tma in **I**, (c) tma in **II** and **III**, and (d) tma in **VI**. Note the differences in the conformation of the tma ligands.

as-synthesized coordination polymers (Figures S3 and S4). In all cases, the main absorption bands are centred around 296 nm, which can be assigned to the ligand-to-metal charge-transfer transition. The additional peaks observed in the compounds **I–VI** can be assigned to the d–d transitions of the Ni^{2+} (d^8) and Co^{2+} (d^7) ions in an octahedral environment. Thus, the peaks at 385, 654, and 737 for **I**, at 384, 653, and 734 for **III**, at 385, 635, and 760 for **IV** and at 404, 678, and 732 for **V** can be assigned to the d–d transitions for Ni^{2+} (d^8), ${}^3\text{A}_{2g} \rightarrow {}^3\text{T}_{2g}$, ${}^3\text{A}_{2g} \rightarrow {}^3\text{T}_{1g}(\text{F})$ and ${}^3\text{A}_{2g} \rightarrow {}^3\text{T}_{1g}(\text{P})$. Similarly, the peaks at 533 and 621 for **II** and at 517 and 615 for **VI** can be assigned to d–d transitions for Co^{2+} (d^7), ${}^4\text{T}_{1g}(\text{F}) \rightarrow {}^4\text{T}_{2g}$ and ${}^4\text{T}_{1g}(\text{F}) \rightarrow {}^4\text{T}_{1g}(\text{P})$.^[30]

Room-temperature solid-state photoluminescence studies were carried out on powdered samples (Perkin–Elmer, U.K.) (Figure 10). The compounds and the sodium salt of tma were excited at 300 nm. The excitation and emission intensities were controlled by using a slit width of 10 nm for both cases. Intense emissions occurring at about 360 nm and about 420 nm were observed, which may be arise from the charge transfer from the ligand to the metal (LMCT band). In addition, bands due to the d–d transitions of the octahedrally coordinated Ni^{2+} (d^8) and Co^{2+} (d^7) are also observed. Thus, the bands at 488 and 526 nm for **I**, 487 and 525 nm for **III**, 427 and 528 for **IV** and 487 and 528 nm for **V** can be assigned to the electronic transitions ${}^3\text{T}_{2g} \rightarrow {}^3\text{A}_{2g}$ and ${}^3\text{T}_{1g}(\text{F}) \rightarrow {}^3\text{A}_{2g}$, respectively, for the Ni^{2+} ion. Similarly, the bands at 486 and 529 nm for **II** and at 486 and 527 nm for **VI** can be assigned to the electronic transitions ${}^4\text{T}_{2g} \rightarrow {}^4\text{T}_{1g}(\text{F})$ and ${}^4\text{T}_{1g}(\text{P}) \rightarrow {}^4\text{T}_{1g}(\text{F})$, respectively, for the Co^{2+} ion.^[30] A study of the literature on the photoluminescence spectra of related compounds reveals that the observed d–d transition bands for the compounds correspond well with those reported for related metal–organic framework compounds.^[29] MOFs based on Co and Ni with 4,4'-oxybis(benzoic acid) and 4,4'-bipyridine, $[\text{Co}_2(\text{C}_{10}\text{H}_8\text{N}_2)][\text{C}_{12}\text{H}_8\text{O}(\text{COO})_2]_2$ and $[\text{Ni}_2(\text{C}_{10}\text{H}_8\text{N}_2)_2][\text{C}_{12}\text{H}_8\text{O}(\text{COO})_2]_2 \cdot \text{H}_2\text{O}$, show LMCT bands at about 440 nm with d–d transition bands at about 480 and about 525 nm, respectively, which are also observed in **I–VI**.

Magnetic Studies

Transition elements possess unpaired electrons and thus provide a useful opportunity for the investigation and correlation of the structure and magnetic behaviour. Transition-metal–organic framework compounds based on trimesic acid^[31] and organic ligands which mimic the symmetry and coordination of trimesic acid^[32] have been prepared and exhibit interesting magnetic behaviour. Thus, $[\text{Mn}_3\{\text{C}_6\text{H}_3(\text{COO})_3\}]$ shows antiferromagnetic behaviour at 5 K,^[31a] and $[(\text{MnCuL})_3\{\text{C}_6\text{H}_3(\text{COO})_3\}](\text{ClO}_4)_3 \cdot 8\text{H}_2\text{O}$ [H_2L = macrocyclic Robson proligand] shows ferromagnetic interaction at 12 K.^[31b] Presently, we have investigated the magnetic susceptibility as a function of temperature for **I–VI** with a SQUID magnetometer in the range 2–300 K by employing a field of 0.1 T (Figures 11 and S5). The observed magnetic moments for compounds **I**, **III**, **IV** and **V**

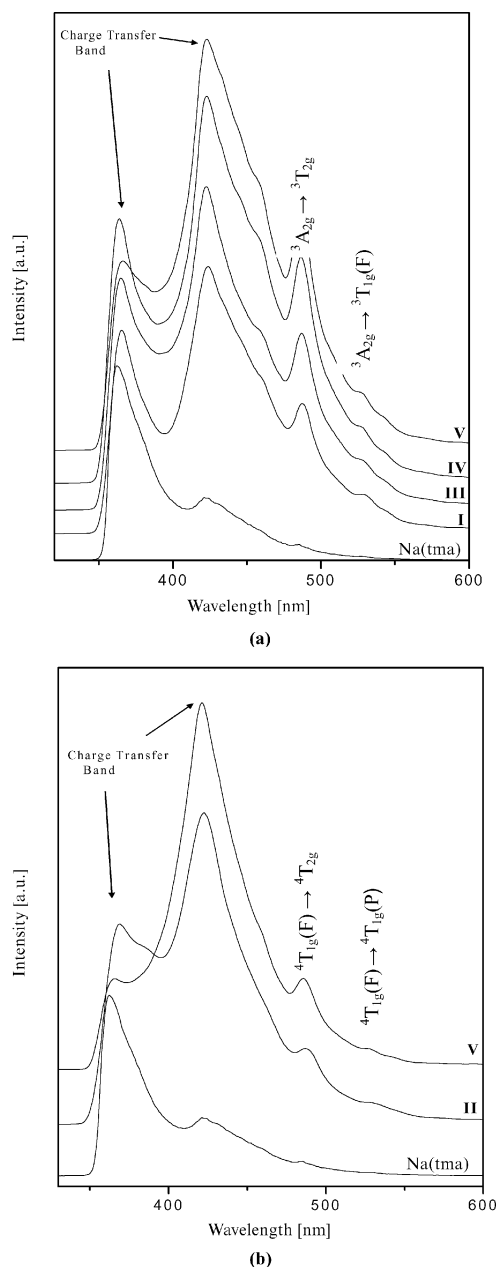


Figure 10. (a) Solid-state photoluminescence spectra of **I**, **III**, **IV**, **V** and Na(tma). (b) Solid-state photoluminescence spectra of **II**, **VI** and Na(tma).

at room temperature (300 K) are 3.07, 3.01, 3.41 and 2.66 μ_B , respectively, which correspond to the non-interacting paramagnetic Ni^{2+} ions and are close to the spin-only magnetic moment of the Ni^{2+} ion in octahedral field (2.83 μ_B). A plot of $1/\chi_M$ vs. T for compounds **III** and **IV** in the temperature range 50–300 K can be fitted to the Curie–Weiss behaviour, with a value for C of 1.46 and 0.89 emu mol^{-1} and for θ_p of -0.7 and 1.8 K, respectively (Figure S5). Similar values have been observed for other compounds.^[33] The presence of Ni–O–Ni dimeric and trimeric units in compounds **I** and **V**, respectively, prompted us to fit the magnetic susceptibility data with a dimer and

trimer model, respectively (Figure 11). The spin Hamiltonian for a Ni^{2+} dimer can be written in the form: $H = -J_{12} \cdot (S_1 \times S_2) - J_{21} \cdot (S_2 \times S_1)$.

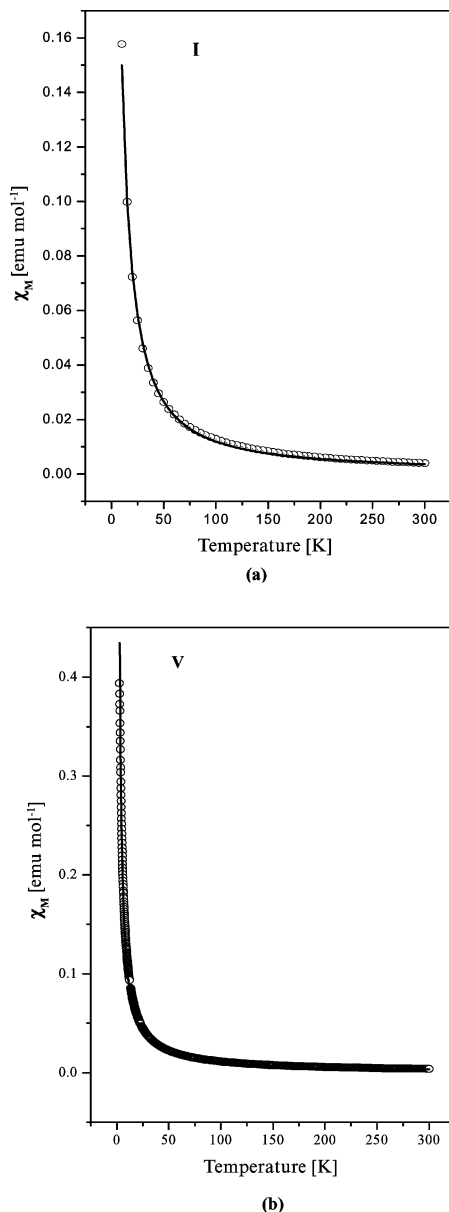


Figure 11. Temperature variation of the molar susceptibility (χ_M) for (a) $[\text{Ni}(\text{C}_{12}\text{N}_2\text{H}_{10})(\text{H}_2\text{O})][\text{C}_6\text{H}_3(\text{COO})_2(\text{COOH})]$ (I) and for (b) $[\text{Ni}_3(\text{H}_2\text{O})_8][\text{C}_6\text{H}_3(\text{COO})_3]$ (V). The symbols correspond to the experimental values, and the theoretical fit is the solid line.

The susceptibility equation for the Ni^{2+} dimer can be obtained by substituting the values for the Ni^{2+} ion in a dimeric complex^[34] into the Van Vleck Equation (1),^[35] where, N_A = Avogadro's number, g = gyromagnetic ratio (approximated here to 2.0), μ_B = Bohr Magnetron, k = Boltzmann constant, T = temperature, $J = J_{12} = J_{21}$ = the coupling constant between two neighbouring metal centres and $x = J/kT$.

$$\chi_M^{\text{dimer}} = \frac{N_A g^2 \mu_B^2}{9kT} \frac{5 + \exp(-5.75x)}{5 + 3\exp(-5.75x) + \exp(-8.63x)} \quad (1)$$

The best fit for the experimentally observed data was obtained with a J value of 11.334 cm^{-1} , which indicates reasonable ferromagnetic interactions. Similarly, for compound V, the spin Hamiltonian for the Ni^{2+} trimer can be written as $H = -J_{12} \cdot (S_1 \times S_2) - J_{23} \cdot (S_2 \times S_3) - J_{13} \cdot (S_1 \times S_3)$. If we consider J_{13} to be equal to zero and $J_{12} = J_{23} = J$, then the susceptibility equation for the Ni^{2+} trimer can be obtained by a similar substitution, as before, of the values of the Ni^{2+} ion in a trimeric complex into Equation (2),^[36] where $x = J/kT$. Here, the best fit for the experimentally observed data gives a J value of 0.3386 cm^{-1} , which indicates much weaker ferromagnetic interactions. The observed magnetic moment for compounds II and VI at 300 K are 4.78 and $4.57 \mu_B$, respectively, which appear to be much larger than the calculated spin only value of $3.87 \mu_B$ for Co^{2+} . This indicates significant orbital contribution. A fit of the $1/\chi_M$ vs. T plot to the Curie–Weiss law, in the temperature range 50–300 K, was linear with a C value of 2.905 and $2.668 \text{ emu mol}^{-1}$ and a θ_P value of -4.99 and -6.45 K , respectively, which indicates weak antiferromagnetic interactions (Figure S5).

$$\chi_M^{\text{trimer}} = \frac{N_A g^2 \mu_B^2}{9kT} \frac{3 + 42\exp(4x) + 18\exp(-2x) + 15\exp(2x) + 3\exp(-6x)}{3 + 7\exp(4x) + 8\exp(-2x) + 5\exp(2x) + 3\exp(-6x) + \exp(-4x)} \quad (2)$$

Conclusions

The immiscible liquid–liquid interphase region has been employed for the preparation of a variety of benzenetricarboxylate coordination polymers of Co and Ni. Most of the prepared compounds have lower-dimensional structures and appear to be stabilized by weak intermolecular forces such as hydrogen bonds or $\pi \cdots \pi$ interactions. Magnetic studies indicate weak ferromagnetic (I, IV and V) as well as antiferromagnetic (II, III and VI) behaviour in these compounds. The present results indicate that it would be profitable to investigate this approach further as it is likely to give better control of the dimensionality of the product phases.

Experimental Section

Synthesis and Initial Characterization: All the compounds were synthesized by employing a biphasic solvothermal reaction involving water and cyclohexanol. The synthesis conditions employed in the present study are presented in Table 3. In a typical synthesis, for I, $\text{Ni}(\text{CH}_3\text{COO})_2 \cdot 4\text{H}_2\text{O}$ (0.2 g, 0.804 mm) was dissolved in H_2O (5 mL), and trimesic acid (0.178 g, 0.804 mm) and 1,10-phenanthroline (0.1602 g, 0.804 mm) were dissolved in cyclohexanol (4 mL) and layered above the aqueous solution. The reaction mixture was placed in a PTFE vessel and sealed in a stainless steel autoclave, heated at $150 \text{ }^\circ\text{C}$ for 3 d and cooled to room temperature in air. The final product contained large quantities of crystals, which were vacuum filtered, washed with deionized water and dried

Table 3. Synthesis conditions for compounds I–VI.

Mol ratio	T [°C]	t [h]	Yield [%]	Product
Ni(CH ₃ COO) ₂ ·4H ₂ O + H ₃ tma + C ₁₂ N ₂ H ₁₀ + 42 C ₆ H ₁₁ OH + 278 H ₂ O	150	72	78	[Ni(C ₁₂ N ₂ H ₁₀)(H ₂ O)]C ₆ H ₃ (COO) ₂ (COOH) (I)
Co(CH ₃ COO) ₂ ·4H ₂ O + H ₃ tma + 0.54 Piperazine + 42 C ₆ H ₁₁ OH + 278 H ₂ O	150	72	72	[Co ₂ (H ₂ O) ₆][C ₆ H ₃ (COO) ₃] ₂ ·(C ₄ N ₂ H ₁₂)(H ₂ O) ₂ (II)
Ni(CH ₃ COO) ₂ ·4H ₂ O + H ₃ tma + 0.54 Piperazine + 42 C ₆ H ₁₁ OH + 278 H ₂ O	150	72	66	[Ni ₂ (H ₂ O) ₆][C ₆ H ₃ (COO) ₃] ₂ ·(C ₄ N ₂ H ₁₂)(H ₂ O) ₂ (III)
Ni(CH ₃ COO) ₂ ·4H ₂ O + H ₃ tma + 2 C ₁₃ N ₂ H ₁₄ + 42 C ₆ H ₁₁ OH + 278 H ₂ O	150	72	78	[Ni(C ₁₃ N ₂ H ₁₄)(H ₂ O)]C ₆ H ₃ (COO) ₂ (COOH) (IV)
Ni(CH ₃ COO) ₂ ·4H ₂ O + H ₃ tma + 42 C ₆ H ₁₁ OH + 278 H ₂ O	150	72	76	[Ni ₃ (H ₂ O) ₈][C ₆ H ₃ (COO) ₃] (V)
Co(CH ₃ COO) ₂ ·4H ₂ O + H ₃ tma + 2 C ₄ N ₂ H ₄ + 42 C ₆ H ₁₁ OH + 278 H ₂ O	150	72	69	[Co(C ₄ N ₂ H ₄)(H ₂ O)]C ₆ H ₃ (COO) ₂ (COOH) (VI)

at ambient conditions. In all cases, the products were found to contain large quantities of single crystals. Thus, greenish-blue squares (I, yield ≈ 78%), pale pink plates (II, yield ≈ 72%), pale green plates (III, yield ≈ 66%), bluish-green blocks (IV, yield ≈ 78%), green blocks (V, yield ≈ 75%) and dark pink rods (VI, yield ≈ 69%) crystals were obtained. I: calcd. C 54.20, N 6.02, H 3.01; found C 54.38, N 6.16, H 2.95%. II, III: calcd. C 34.59, N 3.67, H 4.49; found C 34.21, N 3.82, H 4.20%. IV: calcd. C 54.66, N 5.80, H 4.14; found C 54.58, N 5.92, H 4.25%. V: calcd. C 29.50, H 3.01; found C 29.62, H 3.14%; VI: calcd. C 42.80, N 7.67, H 2.74; found C 42.74, N 7.54, H 2.85%. Powder X-ray diffraction (XRD) patterns were recorded on powdered samples in the 2θ range 5–50° by using Cu-K_α radiation (Philips X'Pert). The XRD patterns were found to be entirely consistent with the simulated XRD patterns generated from the structures determined by single-crystal XRD studies, which establishes the purity of the phases (Figure S6–S11). The thermogravimetric analyses were carried out (Mettler–Toledo) in an oxygen atmosphere (flow rate = 20 mL min⁻¹) in the temperature range 30–800 °C (heating rate = 10 °C min⁻¹). In all cases, the total observed weight loss corresponds well with the loss of the carboxylate and the water molecules 83% (calcd. 84%), 80% (calcd. 80%), 82% (calcd. 81%), 86.5% (calcd. 84.5%), and 79% (calcd. 79.5%) for I, II, III, IV, V and VI, respectively, (Figure S12). The final calcined product was found to be crystalline by powder XRD and corresponds to CoO (JCPDS No. 78-0431) and NiO (JCPDS Nos. 78-0643).

Infrared Spectroscopic Studies: The IR spectra were recorded on KBr pellets (Perkin–Elmer, SPECTRUM 1000). The results indi-

cate characteristic sharp lines with comparable bands (Figure S13 and S14). Minor variations between the bands were noticed between the compounds. The observed bands in compounds I–VI are listed in Table S1. An additional peak at about 1700 cm⁻¹ in the case of I, IV and VI, which corresponds to a –C–O–H vibration, indicates the presence of a free carboxylic acid group in tma; no such bands were observed in II and III.

Single-Crystal Structure Determination: A suitable single crystal of each compound was carefully selected under a polarizing microscope and glued to a thin glass fibre. The single crystal data were collected on a Bruker AXS smart Apex CCD diffractometer at 293(2) K. The X-ray generator was operated at 50 kV and 35 mA by using Mo-K_α (λ = 0.71073 Å) radiation. Data were collected with ω scan width of 0.3°. A total of 606 frames were collected in three different settings of φ (0, 90, 180°) whilst the sample-to-detector distance was fixed at 6.03 cm and the detector position (2θ) fixed at –25°. The data were reduced by using SAINTPLUS,^[37] and an empirical absorption correction was applied by using the SADABS program.^[38] The structure was solved and refined with SHELXL97,^[39] present in the WinGx suit of programs (Version 1.63.04a).^[40] All hydrogen atoms of the carboxylic acids were initially located in the difference Fourier maps, and for the final refinement, the hydrogen atoms were placed in geometrically ideal positions and held in the riding mode. Final refinement included atomic positions for all the atoms, anisotropic thermal parameters for all non-hydrogen atoms and isotropic thermal parameters for all hydrogen atoms. Full-matrix least-squares refinement against |F²| was carried out with the WinGx package of programs.^[40] De-

Table 4. Crystal data and structure refinement parameters for compounds I–VI.^[a]

	I	II	III	IV	V	VI
Empirical formula	C ₂₁ H ₁₄ O ₇ N ₂ Ni	C ₂₂ H ₃₄ O ₂₀ N ₂ Co ₂	C ₂₂ H ₃₄ O ₂₀ N ₂ Ni ₂	C ₂₂ H ₂₀ O ₇ N ₂ Ni	C ₁₈ H ₂₂ O ₂₀ Ni ₃	C ₁₃ H ₁₀ N ₂ O ₇ Co
Formula weight	465.04	764.37	763.89	483.11	732.41	365.16
Crystal system	triclinic	triclinic	triclinic	orthorhombic	triclinic	triclinic
Space group	P $\bar{1}$ (no. 2)	P $\bar{1}$ (no. 2)	P $\bar{1}$ (no. 2)	Pnmm (no. 58)	P $\bar{1}$ (no. 2)	P $\bar{1}$ (no. 2)
a [Å]	9.574(5)	7.1517(12)	7.157(2)	16.390(3)	10.0317(14)	7.140(5)
b [Å]	10.823(6)	10.5393(17)	10.466(3)	18.683(4)	10.0852(14)	9.244(7)
c [Å]	11.175(6)	10.5415(18)	10.495(3)	20.069(4)	13.1549(18)	10.316(7)
α [°]	97.133(9)	110.783(2)	110.779(4)	90.0	75.757(2)	78.091(11)
β [°]	110.790(9)	91.417(3)	92.232(5)	90.0	68.631(2)	88.694(10)
γ [°]	111.831(8)	102.519(2)	101.891(4)	90.0	65.408(2)	79.426(11)
V [Å ³]	960.2(9)	720.7(2)	713.8(4)	6145(2)	1119.9(3)	654.8(8)
Z	2	2	2	8	2	2
T [K]	293(2)	293(2)	293(2)	293(2)	293(2)	293(2)
ρ _{calcd.} [g cm ⁻³]	1.609	1.761	1.777	1.044	2.178	1.852
μ [mm ⁻¹]	1.060	1.247	1.415	0.664	2.604	1.354
Wavelength [Å]	0.71073	0.71073	0.71073	0.71073	0.71073	0.71073
θ range [°]	2.04 to 27.87	2.08 to 28.01	2.09 to 28.00	2.18 to 28.05	1.67 to 28.00	2.02 to 28.11
R index [I > 2σ(I)]	R ₁ = 0.0623 wR ₂ = 0.1544	R ₁ = 0.0360 wR ₂ = 0.0953	R ₁ = 0.0587 wR ₂ = 0.1500	R ₁ = 0.0680 wR ₂ = 0.1686	R ₁ = 0.0398 wR ₂ = 0.0933	R ₁ = 0.0759 wR ₂ = 0.1761
R (all data)	R ₁ = 0.0780 wR ₂ = 0.1656	R ₁ = 0.0413 wR ₂ = 0.0989	R ₁ = 0.0730 wR ₂ = 0.1588	R ₁ = 0.0982 wR ₂ = 0.1878	R ₁ = 0.0489 wR ₂ = 0.0974	R ₁ = 0.1014 wR ₂ = 0.1936

[a] R₁ = Σ|F_o – |F_c||Σ|F_o|; wR₂ = {Σ[w(F_o² – F_c²)]/Σ[w(F_o²)]}^{1/2}. w = 1/[ρ²(F_o)² + (aP)² + bP]. P = [max(F_o, 0) + 2(F_c)²]/3, where a = 0.1017 and b = 0.0000 for I, a = 0.0517 and b = 0.4579 for II, a = 0.0759 and b = 2.0187 for III, a = 0.0990 and b = 3.2207 for IV, a = 0.0391 and b = 0.7381 for V and a = 0.1140 and b = 1.3649 for VI.

tails of the structure solution and final refinements for I–VI are given in Table 4. Selected bond lengths for compounds I–IV and VI are listed in Table 3. CCDC-648864, -648865, -648866, -648867, -648868, -648869 for compounds I–VI contain the crystallographic data for this paper. These data can be obtained free of charge from The Cambridge Crystallographic Data Centre (CCDC) via www.ccdc.cam.ac.uk/data_request/cif.

Supporting Information (see footnote on the first page of this article): UV/Vis spectra of I–VI and of the Na salt of tma, magnetic plots of II, III, IV and VI, simulated and experimental powder X-ray patterns of I–VI, TGA curves of I–VI, IR spectra and data of I–VI and bond angles of I–IV and VI are presented. Diagrams showing the various forms of connectivity of the tma ligand in the compounds and the interactions in VI are also given.

Acknowledgments

SN thanks the Department of Science and Technology (DST), Government of India, BRNS, DAE, Ramanna fellowship (DST) and CSIR for the award of a research grant.

- [1] a) A. C. Sudik, A. P. Côté, A. G. Wong-Foy, M. O. Keeffe, O. M. Yaghi, *Angew. Chem. Int. Ed.* **2006**, *45*, 2528–2533; b) M. Latroche, S. Surblé, C. Serre, C. M. Draznieks, P. L. Llewellyn, J. H. Lee, J. S. Chang, S. H. Jung, G. Férey, *Angew. Chem. Int. Ed.* **2006**, *45*, 8227–8231; c) S. Ma, H. C. Zhou, *J. Am. Chem. Soc.* **2006**, *128*, 11734–11735; d) X. Lin, A. J. Blake, C. Wilson, X. Z. Sun, N. R. Champness, M. W. George, P. Hubberstey, R. Mokaya, M. Schröder, *J. Am. Chem. Soc.* **2006**, *128*, 10745–10753.
- [2] a) Z. T. Yu, Z. L. Liao, Y. S. Jiang, G. H. Li, G. D. Li, J. S. Chen, *Chem. Commun.* **2004**, 1814; b) Z. T. Yu, Z. L. Liao, Y. S. Jiang, G. H. Li, J. S. Chen, *Chem. Eur. J.* **2005**, *11*, 2642; c) F. Gandara, A. Garcia-Cortes, C. Cascales, B. Gomez-Lor, E. Gutierrez-Puebla, M. Iglesias, A. Monge, N. Snejko, *Inorg. Chem.* **2007**, *46*, 3475–3484.
- [3] a) J. B. Livramento, A. Sour, A. Borel, A. E. Merbach, É. Tóth, *Chem. Eur. J.* **2006**, *12*, 989–1003; b) R. Vaidhyanathan, D. Bradshaw, J. N. Rebilly, J. P. Barrio, J. A. Gould, N. G. Berry, M. J. Rosseinsky, *Angew. Chem. Int. Ed.* **2006**, *45*, 6495–6499.
- [4] a) G. Férey, C. M. Draznieks, C. Serre, F. Millange, J. Dutour, S. Surblé, I. Margiolaki, *Science* **2005**, *309*, 2040–2042; b) X. Lin, A. J. Blake, C. Wilson, X. M. Sun, N. R. Champness, M. W. George, P. Hubberstey, R. Mokaya, M. Schröder, D. T. Cramb, G. K. H. Shimizu, *J. Am. Chem. Soc.* **2006**, *128*, 10403–10412; d) A. G. Wong-Foy, A. J. Matzger, O. M. Yaghi, *J. Am. Chem. Soc.* **2006**, *128*, 3494–3495; e) C. N. R. Rao, S. Natarajan, R. Vaidhyanathan, *Angew. Chem. Int. Ed.* **2004**, *43*, 1466–1496; f) X. H. Bu, M. L. Tong, H. C. Chang, S. Kitagawa, S. R. Batten, *Angew. Chem. Int. Ed.* **2004**, *43*, 192–195; g) R. K. Feller, C. N. R. Rao, A. K. Cheetham, *Chem. Commun.* **2006**, 4780–4795; h) D. Maspoch, D. Ruiz-Molina, J. Veciana, *Chem. Soc. Rev.* **2007**, *36*, 770–818.
- [5] a) J. Zhang, Y. Gen Yao, X. Bu, *Chem. Mater.* **2007**, *19*, 5083–5089; b) M. Dinca, J. R. Long, *J. Am. Chem. Soc.* **2007**, *129*, 11172–11176; c) S. R. Halper, L. Do, J. R. Stork, S. M. Cohen, *J. Am. Chem. Soc.* **2006**, *128*, 10745–10753; d) M. Du, Z. H. Zhang, L. F. Tang, X. G. Wang, X. J. Zhao, S. R. Batten, *Chem. Eur. J.* **2007**, *13*, 2578–2586; e) D. R. Xiao, E. B. Wang, H. Y. An, Y. G. Li, Z. M. Su, C. Y. Sun, *Chem. Eur. J.* **2006**, *12*, 6528–6541; f) P. Mahata, A. Sundaresan, S. Natarajan, *Chem. Commun.* **2007**, 4471–4473; g) P. Mahata, D. Sen, S. Natarajan, *Chem. Commun.* **2008**, 1278–1280.
- [6] a) S. M. Humphrey, P. T. Wood, *J. Am. Chem. Soc.* **2004**, *126*, 13236–13237; b) T. C. Stamatatos, D. Foguet-Albiol, S. C. Lee, C. C. Stoumpos, C. P. Raptopoulou, A. Terzis, W. Wernsdorfer, S. O. Hill, S. P. Perlepes, G. Christou, *J. Am. Chem. Soc.* **2007**, *129*, 9484–9499; c) X. M. Zhang, Z. M. Hao, W. X. Zhang, X. M. Chen, *Angew. Chem. Int. Ed.* **2007**, *46*, 3456–3459; d) M. Martinho, D. W. Choi, A. A. DiSpirito, W. E. Antholine, J. D. Semrau, E. Munck, *J. Am. Chem. Soc.* **2007**, *129*, 15783–15785.
- [7] a) J. Zhang, S. Chen, H. Valle, M. Wong, C. Austria, M. Cruz, X. Bu, *J. Am. Chem. Soc.* **2007**, *129*, 14168–14169; b) L. Han, M. C. Hong, R. H. Wang, J. H. Luo, Z. Z. Lin, D. Q. Yuan, *Chem. Commun.* **2003**, 2580–2581; c) J. S. Seo, D. Whang, H. Lee, S. I. Jun, J. Oh, Y. J. Jeon, K. Kim, *Nature* **2000**, *404*, 982–986; d) C. J. Kepert, T. J. Prior, M. J. Rosseinsky, *J. Am. Chem. Soc.* **2000**, *122*, 5158–5168.
- [8] G. Férey, *Chem. Soc. Rev.* **2008**, *37*, 191–214.
- [9] a) L. Xu, E. Y. Choi, Y. U. Kwon, *Inorg. Chem.* **2008**, *47*, 1907–1909; b) Q. Fang, G. Zhu, M. Xue, Z. Wang, J. Sun, S. Qiu, *Cryst. Growth Des.* **2008**, *8*, 319–329; c) F. Luo, Y. X. Che, J. M. Zheng, *Cryst. Growth Des.* **2008**, *8*, 176–178; d) A. M. Kirillov, Y. Y. Karabach, M. Haukka, M. F. C. G. da Silva, J. Sanchiz, M. N. Kopylovich, A. J. L. Pombeiro, *Inorg. Chem.* **2008**, *47*, 162–175; e) L. Xu, E. Y. Choi, Y. U. Kwon, *Inorg. Chem.* **2008**, *47*, 10670–10680; f) M. Du, X. J. Jiang, X. J. Zhao, *Inorg. Chem.* **2006**, *45*, 3998–4006.
- [10] a) S. O. H. Gutschke, M. Molinier, A. K. Powell, R. E. P. Wippeny, P. T. Wood, *Chem. Commun.* **1996**, 823–824; b) S. S. Y. Chui, S. M. F. Lo, J. P. H. Charmant, A. G. Orpen, I. D. Williams, *Science* **1999**, *283*, 1148–1150; c) J. Kim, B. Chen, T. M. Reineke, H. Li, M. Eddaoudi, D. B. Moler, M. O. Keeffe, O. M. Yaghi, *J. Am. Chem. Soc.* **2001**, *123*, 8239–8247; d) M. Pasqu, F. Lloret, N. Avarvari, M. Julve, M. Andruh, *Inorg. Chem.* **2004**, *43*, 5189–5191; e) Z. Li, G. Zhu, X. Guo, X. Zhao, Z. Jin, S. Qiu, *Inorg. Chem.* **2007**, *46*, 5174–5178; f) X. Guo, G. Zhu, Z. Li, Y. Chen, X. Li, S. Qiu, *Inorg. Chem.* **2007**, *46*, 4065–4070.
- [11] a) D. N. Dybtsev, H. Chun, K. Kim, *Chem. Commun.* **2004**, 1594–1595; b) K. Jin, X. Huang, L. Pang, J. Li, A. Appel, S. Wherland, *Chem. Commun.* **2002**, 2872–2873; c) J. H. Liao, P. C. Wu, Y. H. Bai, *Inorg. Chem. Commun.* **2005**, *8*, 390–393; d) Z. Lin, D. S. Wragg, R. E. Morris, *Chem. Commun.* **2006**, 2021–2023.
- [12] a) P. M. Forster, A. K. Cheetham, *Angew. Chem. Int. Ed.* **2002**, *41*, 457–459; b) P. M. Forster, P. M. Thomas, A. K. Cheetham, *Chem. Mater.* **2002**, *14*, 17.
- [13] a) K. P. Kalyanikutty, U. K. Gautam, C. N. R. Rao, *Solid State Sci.* **2006**, *8*, 296–302; b) M. Ghosh, U. K. Gautam, V. V. Agarwal, G. U. Kulkarni, C. N. R. Rao, *J. Colloid Interf. Sci.* **2005**, *289*, 305–318; c) U. K. Gautam, M. Ghosh, C. N. R. Rao, *Langmuir* **2004**, *20*, 10775–10778; d) M. K. Sanyal, V. V. Agrawal, M. K. Bera, K. P. Kalyanikutty, J. Dailant, C. Blot, S. Kubowicz, O. Kononov and C. N. R. Rao, *J. Phys. Chem. C.* **2008**, DOI: 10.1021/jp710635e.
- [14] J. Kim, B. Chen, T. M. Reineke, H. Li, M. Eddaoudi, D. B. Moler, M. O. Keeffe, O. M. Yaghi, *J. Am. Chem. Soc.* **2001**, *123*, 8239–8247.
- [15] M. J. Plater, M. R. S. J. Foreman, R. A. Howie, J. M. S. Skakle, E. Coronado, C. J. Gomez-Garcia, T. Gelbrich, M. B. Hursthouse, *Inorg. Chim. Acta* **2001**, *319*, 159–175.
- [16] a) J. Y. Han, W. Y. Wei, *Acta Crystallogr., Sect. E* **2005**, *61*, m2242–m2243; b) W. Wei, Y. Dong, J. Han, H. Chang, *Acta Crystallogr., Sect. E* **2006**, *62*, m26–m27.
- [17] a) L. S. Long, Y. R. Wu, R. B. Huang, L. S. Zheng, *Inorg. Chem.* **2004**, *43*, 3798–3800; b) S. K. Ghosh, P. K. Bharadwaj, *Angew. Chem. Int. Ed.* **2004**, *43*, 3577–3580; c) B. Zhao, P. Cheng, X. Chen, C. Cheng, W. Shi, D. Liao, S. Yan, Z. Jiang, *J. Am. Chem. Soc.* **2004**, *126*, 3012–3013.
- [18] *Gaussian 98, Revision A. 11*, Gaussian Inc., Pittsburgh, PA, **2001**.
- [19] S. Schneider, *Hydrogen-Bonding: A Theoretical Perspective*, Oxford University Press, Oxford, **1997**.

- [20] G. R. Desiraju, T. Steiner, *The Weak Hydrogen Bond*, Oxford University Press, Oxford, **1999**.
- [21] S. Noro, T. Akutagawa, T. Nakamura, *Cryst. Growth Des.* **2007**, *7*, 1205–1208.
- [22] M. J. Plater, M. R. S. J. Foreman, E. Coronado, C. J. Gómez-García, A. M. Z. Slawin, *J. Chem. Soc., Dalton Trans.* **1999**, 4209–4216.
- [23] T. L. Groy, H. Li, O. M. Yaghi, *J. Am. Chem. Soc.* **1996**, *118*, 9096–9101.
- [24] F. A. P. Paz, J. Klinowski, *Inorg. Chem.* **2004**, *43*, 3882–3893.
- [25] E. Y. Choi, K. Young-Uk, *Inorg. Chem.* **2005**, *44*, 538–545.
- [26] a) W. D. Cheng, D. S. Wu, J. Shen, S. P. Huang, Z. Xie, H. Zhang, Y. J. Gong, *Chem. Eur. J.* **2007**, *13*, 5151–5159; b) C. B. Aakeroy, N. Schultheiss, J. Desper, *Inorg. Chem.* **2005**, *44*, 4983–4991; c) E. Tynan, P. Jensen, A. C. Lees, B. Moubaraki, K. S. Murray, P. E. Kruger, *Cryst. Eng. Commun.* **2005**, 90–95; d) T. J. Prior, D. Bradshaw, S. J. Teat, M. J. Rosseinsky, *Chem. Commun.* **2003**, 500–501.
- [27] G. R. Desiraju, *Angew. Chem. Int. Ed. Engl.* **1995**, *34*, 2311–2327.
- [28] L. Brammer, J. C. M. Rivas, R. Atencio, S. Fang, F. C. Pigge, *J. Chem. Soc., Dalton Trans.* **2000**, 3855–3867.
- [29] P. Mahata, G. Madras, S. Natarajan, *J. Phys. Chem. B* **2006**, *110*, 13759–13768.
- [30] A. B. P. Lever, *Inorganic Electronic Spectroscopy*, Elsevier, New York, **1968**.
- [31] a) S. O. H. Gutschke, M. Molinier, A. K. Powell, R. E. P. Winpenny, P. T. Wood, *Chem. Commun.* **1996**, 823–824; b) M. Pascu, F. Lloret, N. Avarvari, M. Julve, M. Andruh, *Inorg. Chem.* **2004**, *43*, 5189–5191.
- [32] a) D. Maspoche, N. Domingo, D. Ruiz-Molina, K. Wurst, J. Tejada, C. Rovira, J. Veciana, *Chimie* **2005**, *8*, 1213–1225; b) F. Luo, J. M. Zheng, M. Kurmoo, *Inorg. Chem.* **2007**, *46*, 8448–8450.
- [33] J. N. Behera, C. N. R. Rao, *J. Am. Chem. Soc.* **2006**, *128*, 9334–9335.
- [34] P. W. Ball, A. B. Blake, *J. Chem. Soc. A* **1969**, 1415–1422.
- [35] O. Kahn, *Molecular Magnetism*, VCH Publishers, Weinheim, **1993**.
- [36] F. J. Rietmeijer, G. A. Van Albada, R. A. G. De Graff, J. G. Haasnoot, J. Reedijk, *Inorg. Chem.* **1985**, *24*, 3597–3601.
- [37] SMART (V 5.628), SAINT (V 6.45a), XPREP, SHELXTL, Bruker AXS Inc., Madison, Wisconsin, USA, **2004**.
- [38] G. M. Sheldrick, *Siemens Area Correction Absorption Correction Program*, University of Göttingen, Göttingen, Germany, **1994**.
- [39] G. M. Sheldrick *SHELXL-97 Program for Crystal Structure Solution and Refinement*, University of Göttingen, Göttingen, Germany, **1997**.
- [40] WinGx Suite for small molecule single-crystal crystallography: J. L. Farrugia, *J. Appl. Crystallogr.* **1999**, *32*, 837–838.

Received: February 9, 2008

Published Online: June 25, 2008